Chem

CellPress

Article

Charge Transfer between [4Fe4S] Proteins and DNA Is Unidirectional: Implications for Biomolecular Signaling

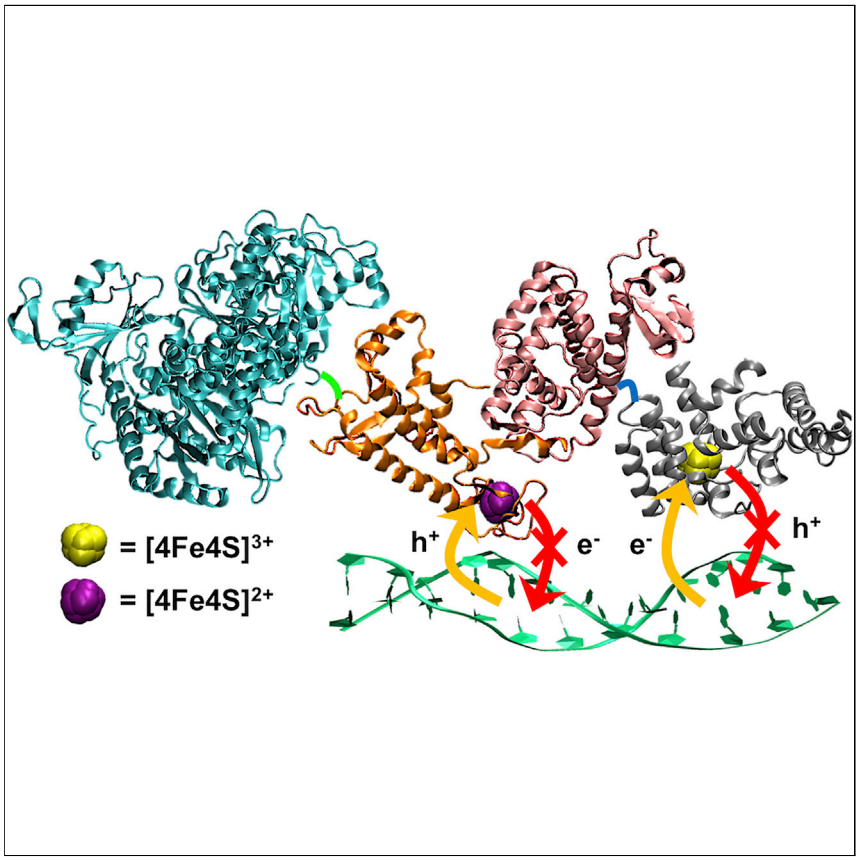

Understanding molecular signaling mechanisms in cells is critically important to biology and medicine. A prominent case is the search for drug targets in cancer signaling pathways. Recently, it was proposed that charge transfer through DNA may enable signaling between iron-sulfur proteins involved in DNA repair and replication. We show that exclusive DNA mediation is energetically unfavorable and kinetically unfeasible, but redox agents might assist the protein signaling. Our analysis narrows the range of possible charge transfer-based mechanisms for intracellular signaling.

Ruijie D. Teo, Benjamin J.G. Rousseau, Elizabeth R. Smithwick, Rosa Di Felice, David N. Beratan, Agostino Migliore

agostino.migliore@duke.edu

HIGHLIGHTS

Charge transfer between [4Fe4S] proteins and DNA is unidirectional

DNA charge transport is not sufficient to enable signaling between [4Fe4S] proteins

Redox agents in the cell may aid DNA in carrying out charge transfer-based signaling

Teo et al., Chem 5, 122–137
January 10, 2019
https://doi.org/10.1016/j.chempr.2018.09.026

Chem

CellPress

Article

Charge Transfer between [4Fe4S] Proteins and DNA Is Unidirectional: Implications for Biomolecular Signaling

Ruijie D. Teo,[1] Benjamin J.G. Rousseau,[1] Elizabeth R. Smithwick,[1] Rosa Di Felice,[2,3,4] David N. Beratan,[1,5,6] and Agostino Migliore[1,7,*]

SUMMARY

Recent experiments suggest that DNA-mediated charge transport might enable signaling between the [4Fe4S] clusters in the C-terminal domains of human DNA primase and polymerase α, as well as the signaling between other replication and repair high-potential [4Fe4S] proteins. Our theoretical study demonstrates that the redox signaling cannot be accomplished exclusively by DNA-mediated charge transport because part of the charge-transfer chain has an unfavorable free energy profile. We show that hole or excess electron transfer between a [4Fe4S] cluster and a nucleic acid duplex through a protein medium can occur within microseconds in one direction while it is kinetically hindered in the opposite direction. We present a set of signaling mechanisms that may occur with the assistance of oxidants or reductants, using the allowed charge-transfer processes. These mechanisms would enable the coordinated action of [4Fe4S] proteins on DNA, engaging the [4Fe4S] oxidation state dependence of the protein-DNA binding affinity.

INTRODUCTION

Many DNA repair and replication enzymes contain [4Fe4S] clusters,[1,2] and experiments suggest a key role for these clusters in regulating enzyme activity.[3,4] For example, in [4Fe4S]-containing base excision repair enzymes such as endonuclease III (EndoIII) and MutY, charge transfer (CT) from one [4Fe4S] cluster to the other, mediated by DNA, could exchange the redox states of the two clusters, thus establishing a "communication" between the two proteins that enables the coordination of their DNA-repair activities.[5–7] In this scenario, a disruption of the DNA nucleobase pairing would inhibit the charge transport and therefore the signaling between EndoIII and MutY. DinG, an R-loop repairing helicase, is thought to cooperate with base excision repair enzymes (to detect R loops in DNA) through a similar mechanism.[8] A recent study demonstrated that various repair and replication proteins with high-potential [4Fe4S] clusters undergo a significant increase in their DNA binding affinity when their clusters are oxidized.[9] In particular, the [4Fe4S]-containing C-terminal domain of primase large subunit (p58c) binds DNA tightly when the [4Fe4S] cluster is oxidized, while the protein and DNA are more loosely associated when the cluster is reduced (as shown in terms of protein redox inactivity on DNA-modified electrodes[4]). This finding suggests a mechanism based on DNA-mediated charge transport for the handoff of the DNA template/RNA primer from p58c to Polα, which is required to initiate DNA replication.[4]

The proposed handoff mechanism is preceded by the oxidation of the [4Fe4S] cluster in p58c by the DNA, which enables tight p58c binding to the RNA/DNA duplex.

The Bigger Picture

We investigate the role of DNA mediation in redox signaling processes between [4Fe4S] clusters that are relevant to DNA replication and repair. Through kinetic modeling, electronic structure calculations, and thermodynamic analysis, our theoretical study demonstrates that charge transfer between a [4Fe4S] cluster and a nucleic acid duplex bound to the [4Fe4S] protein is unidirectional. This unidirectionality implies that the DNA mediation of biological redox signaling needs to be assisted by charge injection into the duplex from cellular oxidants or reductants. Using this important mechanistic implication and the dependence of DNA binding affinity on the charging state of the [4Fe4S] cluster, we identify a set of possible mechanisms, based on charge transfer, for redox signaling between high-potential [4Fe4S] proteins involved in DNA replication and repair. Our analysis of these signaling mechanisms fosters experimental studies of functional charge transfer in [4Fe4S] protein systems.

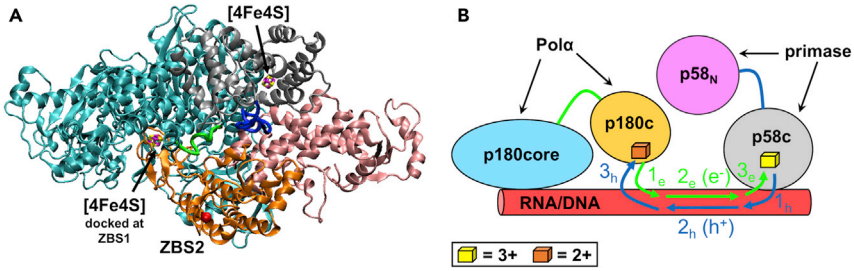

Figure 1. Human Primosome-Nucleic Acid Complex

(A) Portion of the primosome crystal structure (PDB: 5EXR[12]) highlighting the [4Fe4S] cluster docked to p180c (at zinc binding site 1, ZBS1) relative to p58c [4Fe4S] cluster and to the other zinc binding site (ZBS2) in p180c. Color code: Zn (red), S (yellow), Fe (magenta), p180core (cyan), p180c (orange), p58c (silver), $p58_N$ (pink), p180core-p180c linker (green), p58c-$p58_N$ linker (blue).

(B) Schematic view of the protein complex bound to RNA/DNA. p58c, with an oxidized [4Fe4S] cluster (yellow), is linked to primase N-terminal domain ($p58_N$). $p58_N$ connects primase to Polα. We show the catalytic core (p180core) linked to the C-terminal subunit p180c of Polα, and a [4Fe4S] cluster (orange) bound to p180c. The nucleic acid transiently associates primase and Polα. The distance between the p180c [4Fe4S] cluster and the duplex depends on the conformation of the p180core-p180c linker. The p58c [4Fe4S] cluster is at edge-to-edge distances of 50.9 Å and 38.6 Å from ZBS2 and from the [4Fe4S] cluster docked to p180c, respectively. For hole transport exclusively mediated by the duplex, the path of the charge from one [4Fe4S] cluster to the other would consist of: step 1_h from the initially oxidized iron-sulfur cluster in p58c (oxidation state 3+, represented as a yellow cube) to the duplex, through the protein medium; step 2_h, namely, the injected hole, h^+, moves across the duplex; step 3_h from the duplex to the cluster in p180c, which may occur with or without protein mediation depending on the protein arrangement in Polα and the positioning of the duplex. In the case of excess electron transport, the CT path would be as follows: the initially reduced p180c cluster (oxidation state 2+, represented as on orange cube) injects an electron, e^-, into the initially neutral duplex; the excess electron transfers to the nucleic acid portion close to Polα (step 2_e); the electron is donated from the anionic duplex to p58c (step 3_e).

The electron-hole transfer from the duplex to the [4Fe4S] cluster is proposed to be mediated by the Y309, Y345, and Y347 residues.[4] When the nascent duplex is long enough to approach a nearby Polα (Figure 1), a hole can move from the p58c cluster, across the duplex, to Polα, which is assumed to contain an iron-sulfur cluster.[10] The transferring charge may be an electron hole or an excess electron. The hole should first be transferred from the $[4Fe4S]^{3+}$ cluster anchored to p58c, through the protein, to the initially neutral DNA/RNA duplex (step 1_h in Figure 1B, which injects the hole h^+ in the nucleic acid). After charge transport across the transiently oxidized duplex (step 2_h in Figure 1B), the hole should be delivered to the initially reduced iron-sulfur cluster, $[4Fe4S]^{2+}$, on Polα (step 3_h in Figure 1B). Clearly, the DNA-mediated charge transport from one cluster to the other can be seen as the motion of an electron in the opposite direction in the oxidized protein-nucleic acid system. This duplex-mediated CT switches the oxidation states of the iron-sulfur clusters in the two enzymes (and therefore their relative binding affinities to the duplex), resulting in a reduced iron-sulfur cluster on p58c and an oxidized $[4Fe4S]^{3+}$ cluster on Polα. Thus, the charge transport establishes a signal that promotes the primer dissociation from primase (primer truncation) and its association with Polα (handoff to Polα).[4] If the transport of an excess electron is at play (in a reduced protein-nucleic acid system), the excess electron first transfers from the initially reduced iron-sulfur cluster on Polα to the duplex (step 1_e in Figure 1B). After moving across the (transiently anionic) duplex (step 2_e), the excess electron charge is donated to the initially oxidized iron-sulfur cluster in p58c (step 3_e in Figure 1B). Similar considerations apply to the DNA-mediated charge transport in the redox signaling between other [4Fe4S] proteins involved in DNA repair and replication.[5–7,9,11] Therefore, assessing the

[1]Department of Chemistry, Duke University, Durham, NC 27708, USA

[2]Department of Physics and Astronomy, University of Southern California, Los Angeles, CA 90089, USA

[3]Department of Biological Sciences (Quantitative and Computational Biology Section), University of Southern California, Los Angeles, CA 90089, USA

[4]Istituto Nanoscienze, Consiglio Nazionale delle Ricerche (CNR-NANO), Via Campi 213/A, 41125 Modena, Italy

[5]Department of Physics, Duke University, Durham, NC 27708, USA

[6]Department of Biochemistry, Duke University, Durham, NC 27710, USA

[7]Lead Contact

*Correspondence: agostino.migliore@duke.edu

https://doi.org/10.1016/j.chempr.2018.09.026

feasibility of a signaling mechanism based on nucleic acid-mediated charge transport can have far-reaching implications for our understanding of biological signaling and drug targets in cancer signaling pathways.[3,11]

The redox signaling mechanism proposed by O'Brien et al.[4] is the subject of debate.[4,13–15] A major criticism of this mechanism arises from the fact that O'Brien et al.[4] used a partially misfolded p58c in their study.[16] Use of wild-type p58c should exclude Y345 and Y347 from participating in strong CT pathways between the [4Fe4S] cluster and the duplex[12,17] and would suggest a different explanation for the findings of O'Brien et al.[13,14] Furthermore, a different mechanism was proposed for the primer synthesis, in which p58c motion, rather than a charge-transfer mechanism, is responsible for both the termination of the primer synthesis and its loading to Polα.[12]

The available experimental evidence cannot rule out either of the two proposed primer truncation/handoff mechanisms. The primosome structure is certainly compatible with the mechanism based on p58c motion,[12] although the cause of p58c rotation that brings the nascent primer into contact with the p180core is not yet fully understood. Experimental data on repair and replication proteins are also compatible with a mechanism based on DNA-mediated CT between [4Fe4S] clusters.[4,9,11] Ultimately, the function of [4Fe4S] clusters as redox switches using DNA charge transport may coexist and operate concertedly with protein motion to coordinate primase and Polα action on the primer.

DNA-mediated redox communication between [4Fe4S] clusters offers an appealing and broadly relevant protein signaling paradigm, which could indeed be at play in DNA replication and lesion detection/repair processes. The feasibility of such signaling (irrespective of the specific CT pathway) on biologically relevant timescales is the central question of biological and biomedical significance. This question did not find an answer in the outlined debate. The answer requires demonstrating whether CT between a high-potential [4Fe4S] cluster and RNA/DNA is energetically accessible, and therefore kinetically feasible, in both directions (Figure 2). In fact, irrespective of whether an electron hole or an excess electron is transferring, the redox signaling between the two [4Fe4S] clusters requires charge transfer from one cluster to the nucleic acid duplex (CT in the cluster-to-duplex direction, namely, step 1_h or 1_e in Figure 1B), followed by charge transport through the duplex (step 2_h or 2_e, both of which have been widely studied in the literature[11]), and finally charge transfer from the duplex to the other [4Fe4S] cluster (CT in the duplex-to-cluster direction, namely, step 3_h or 3_e in Figure 1B). Here we will answer this question, showing that through-protein charge transfer between a high-potential [4Fe4S] cluster and a nucleic acid duplex is unidirectional, and therefore one of the two required CT processes between [4Fe4S] cluster and duplex is kinetically unfeasible (Figure 2A; also see steps 1_h and 1_e in Figure 1B). This result significantly delimits the possible realizations of DNA charge transfer-mediated redox signaling between [4Fe4S] proteins. We propose a general set of possible signaling mechanisms that are based upon [4Fe4S] redox state switching and the unidirectional character of the cluster-duplex CT (Figure 2).

RESULTS AND DISCUSSION

System Structure and Modeling

To study the redox signaling between iron-sulfur proteins, we need to fill a gap in the structural information available from the literature, which partially endows our study with a predictive aim, thus fostering future experimental studies that may assess our

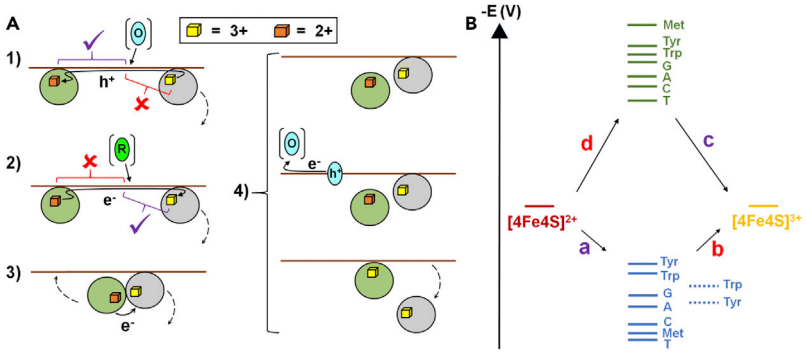

Figure 2. CT-Mediated [4Fe4S] Protein Signaling and Pertinent Redox Potentials

(A) Possible mechanisms for protein communication via CT, supported by the primer: (1) hole transfer or (2) excess electron transfer between the p58c and p180c [4Fe4S] clusters (drawn as small cubes), mediated by an RNA/DNA duplex transiently bound to both p58c and p180core. Part of the CT route (in red) is energetically unfavorable. Nearby oxidants (O) or reductants (R) should support these signaling mechanisms. (3) Change in relative DNA binding affinities of primase and Polα caused by direct inter-cluster CT. (4) Competitive protein binding to the primer, modulated by sequential changes in the [4Fe4S] cluster oxidation states assisted by RNA/DNA and surrounding redox agents.

(B) Redox potential landscape (Table S1) for hole transfer (blue) and excess electron transfer (green), and related downhill (a, c) and uphill (b, d) electron transfer processes. Mechanism 1 would first require hole hopping from $[4Fe4S]^{3+}$ in p58c to the duplex through protein redox-active residues. However, the hole transfer to any amino acid (that is, the electron-transfer step b in the opposite direction) is energetically uphill, thus making the hole-hopping process kinetically unfeasible (forbidden step in mechanism 1). If the duplex is oxidized by an external agent (O), the hole can be delivered to $[4Fe4S]^{2+}$ in p180c, that is, an electron can transfer downhill in the opposite direction (step a), from the $[4Fe4S]^{2+}$ energy level to one of the duplex energy levels, possibly occupying intermediate Tyr and Trp levels. Mechanism 2 would first require direct or protein-mediated electron transfer from $[4Fe4S]^{2+}$ in p180c to the duplex (uphill step d, that is, kinetically unfeasible step in mechanism 2). However, if the duplex is negatively charged by an external agent (R), the excess electron can move downhill from any of the purine energy levels, through Tyr and Trp levels, to reduce the initially oxidized p58 cluster (allowed electron transfer step c). The dashed blue lines correspond to different choices for Tyr and Trp oxidation potentials that are described in the main text.

conclusions. Although eukaryotic DNA polymerases need [4Fe4S] clusters to form active complexes,[10] crystallization of Polα with the cluster is hindered by the lability of the latter, which is expected to bind p180c at the solvent-exposed zinc binding site 1 (ZBS1).[10,12] Thus, we docked a [4Fe4S] cluster to Polα at ZBS1 (see Theoretical and Computational Procedures and Section S1 in Supplemental Information). Compared with the other zinc binding site ZBS2 in p180c, ZBS1 is closer to the p58c [4Fe4S] cluster and is proximal to the Polα DNA binding catalytic core (Figure 1). The crystal structure with PDB: 4QCL[18] also shows that ZBS1 is close to W1084 and to Tyr residues near the duplex (Figure S2) that may assist CT between the cluster and the duplex.

Signaling exclusively mediated by CT through DNA[4] requires a $[4Fe4S]^{3+}$ cluster in p58c to oxidize the duplex and then a $[4Fe4S]^{2+}$ cluster in Polα to reduce the duplex, by means of hole or excess electron transport (Figures 1B and 2). For any DNA-mediated CT path, the inter-cluster distance would be prohibitively long for single-step charge self-exchange between the iron-sulfur clusters in p58c and p180c. Instead (in the case of hole transfer, for example), the initially oxidized [4Fe4S] cluster in p58c should oxidize the duplex, assisted by redox-active Tyr, Trp, and Met[19,20] residues. Then, hole transfer through the RNA/DNA duplex should bring the hole sufficiently close to Polα to enable its transfer to the p180c [4Fe4S] cluster, by hopping

through Polα or by direct tunneling. Aligning the p180core crystal structure (PDB: 5EXR[12]) with the docked [4Fe4S] cluster to the crystal structure of a p180core-RNA/DNA complex (PDB: 4QCL[18]), we found that the [4Fe4S] cluster can directly face the duplex, depending on the p180c-linker-p180core conformation. Therefore, if this theoretical result is validated by future experiments, it means that the charge can also transfer directly between the duplex and the [4Fe4S] cluster in p180c.

CT between [4Fe4S] Cluster and Nucleic Acid

After identifying all of the redox-active residues[19,20] in the primosome that may support charge hopping (Figure S3), we studied the feasibility of the CT steps involved in signaling mechanisms 1 and 2 (Figure 2A) without the intervention of external redox agents in the cell environment, namely: charge hopping from the [4Fe4S] cluster of a protein to the nucleic acid duplex, followed by charge transport through the duplex toward its contact with the other protein and CT from the thus charged duplex to the [4Fe4S] cluster on the other protein, directly or via hopping through the pertinent protein medium.

The charge transport through the duplex, which is step 2_h or 2_e in Figure 1B, should consist of no more than eight charge-hopping steps through the nine base pairs of the optimal-length nucleic acid duplex[12] shared by the two proteins before the duplex handoff to p180c. However, the number of hopping steps required to traverse the duplex can be less than eight, depending on which purine nucleobases are involved in the protein-nucleic acid contact regions. In addition, structural constraints on the duplex bound to the proteins may reduce the reorganization energies associated with the charge hopping through the nucleic acid compared with the values expected in solution.[21–23] Even without considering the enhancement in rapidity of DNA charge transport that may result from these two factors and from the occurrence of CT mechanisms with slow distance dependence of the effective CT rate,[24,25] the charge transfer across the DNA template/RNA primer can always take place within the biologically relevant millisecond timescale, as is easily seen by describing the hopping steps with Marcus' CT rate equation and using values from the literature for the free energy parameters[21–23,26–28] and electronic couplings that mainly involve guanine (for hole transfer)[29–32] or thymine (for excess electron transfer).[33] Therefore, we will not consider further the DNA charge transport, and our analysis will focus on the protein-mediated CT between the iron-sulfur clusters and the nucleic acid, namely, the two fundamental steps drawn for the CT-mediated signaling mechanisms 1 and 2 of Figure 2A.

We begin our analysis with the CT from the [4Fe4S] cluster in p58c to a bound template/primer duplex. This CT would be the first essential step in a p58c-p180c signaling mechanism that is based on duplex-mediated CT between their iron-sulfur clusters. First, we inspected the electron tunneling pathways between the iron-sulfur cluster and RNA/DNA duplex in a p58c-duplex complex (PDB: 5F0Q[12]). Our pathway analysis (Supplemental Information [Section S6] and Figure S4) indicated that the strongest tunneling pathways terminate on the DA10, DA7, and guanosine triphosphate (GTP) purine nucleobases (see Figure S4, as well as Figures 3 and 5). Charge tunneling to DA10 is fast (Tables S5 and S6), but we excluded DA10 as a possible hole donor in hole transfer, or electron donor in excess electron transfer, for signaling purposes. In fact, DA10 lies in the single-stranded DNA portion, and the next charge transport through the DNA needed for signaling would be kinetically unfeasible.[34,35] DA7 also lies in the DNA single strand. However, DA7 is H-bonded to H303, and the DA7-H303 pair is π-stacked to the GTP-DC6 pair at a terminus of the RNA/DNA duplex. Thus, DA7-H303 behaves as a pseudo pair that extends the

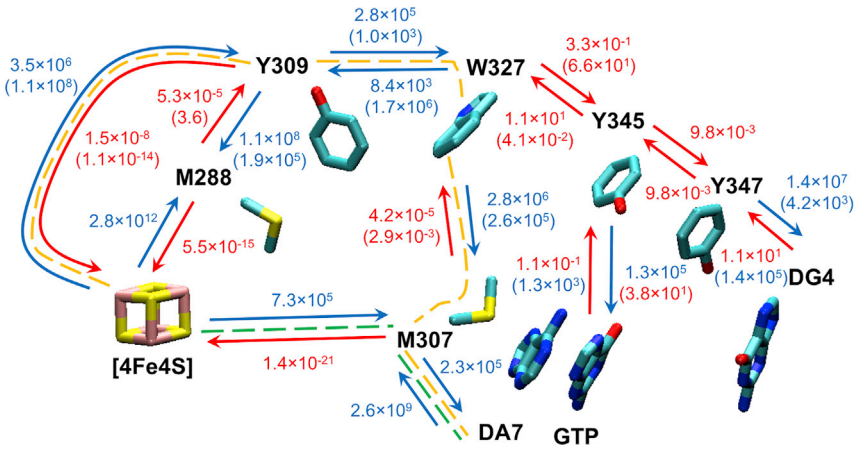

Figure 3. CT Steps and Rate Constants (in s^{-1}) in Hole Hopping between the Iron-Sulfur Cluster and the Nucleobases in the p58c-RNA/DNA Complex (Crystal Structure with PDB: 5F0Q)

The CT steps with an inverse rate constant within a biologically relevant millisecond timescale are in blue; the other steps are in red. The fastest (second fastest) CT route is drawn as a green (orange) dashed line. Possible routes for charge transport between the [4Fe4S] cluster and the nucleic acid are **1**: [4Fe4S]-M307-DA7; **2**: [4Fe4S]-Y309-W327-M307-DA7; **3**: [4Fe4S]-Y309-W327-Y345-GTP; **4**: [4Fe4S]-Y309-W327-Y345-Y347-DG4; **5**: [4Fe4S]-M288-Y309-W327-M307-DA7; **6**: [4Fe4S]-M288-Y309-W327-Y345-GTP; **7**: [4Fe4S]-M288-Y309-W327-Y345-Y347-DG4.

double-stranded region (Figure S4). In the p58-nucleic acid complex, the distances from the [4Fe4S] cluster to DA7 and GTP are such that the pertinent tunneling pathways are not kinetically competitive with the connecting charge-hopping routes investigated below. Yet the DA7 and GTP purines also are at shorter geometric distances from the iron-sulfur cluster than other purine nucleobases in the DNA/RNA duplex segment. Thus, simple structural analysis also suggests the DA7 and GTP purines as preferential sites for CT to/from the iron-sulfur cluster via charge hopping through intervening redox-active amino acid residues. We also included DG4 in our analysis, since this is the closest guanine to Y347 and would be the most probable electron acceptor in a hopping chain that contains the Tyr residues investigated by O'Brien et al.[4]

Next, we analyze the feasibility of hole transfer between the iron-sulfur cluster bound to p58c and the duplex in either direction. We will show that: (1) a hole can transfer from an initially oxidized duplex to an initially reduced iron-sulfur cluster, $[4Fe4S]^{2+}$ (namely, in terms of electron transfer, an electron can be donated by the cluster to the nucleic acid), thus leading to a neutral duplex and $[4Fe4S]^{3+}$ on p58c; (2) on the contrary, the hole cannot transfer in the opposite direction, from an initially oxidized cluster to an initially neutral nucleic acid, thus leading to $[4Fe4S]^{2+}$ and an oxidized duplex (step 1_h in Figure 1B, or step b of Figure 2B, as described in terms of electron transfer in the opposite direction and, partly, in terms of energetics). This is the forbidden step in signaling mechanism 1 (Figure 2A).

Inspecting the crystal structure of the human primosome (see Figure S3), we identified M288, Y309, W327, and M307 as the p58c residues that can be involved in the hole transfer from the RNA/DNA duplex to $[4Fe4S]^{2+}$. We inspected the entire network of hole-transfer routes through these residues, using the Marcus rate constant expression for nonadiabatic electron transfer[36] to quantify the speed of the individual hole-transfer steps. The electronic couplings and free energies entering the CT rate constants were calculated as described in Theoretical and Computational

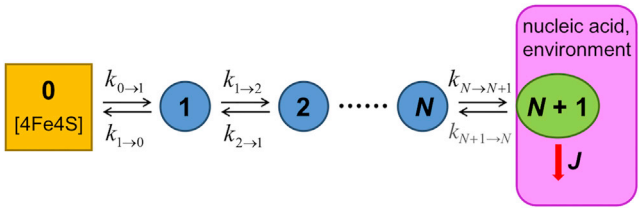

Figure 4. Kinetic Model for Electron Transfer from the [4Fe4S] Cluster in p58c to the Anchored Nucleic Acid

0 is the iron-sulfur cluster; 1 to *N* denote the primase redox-active residues that intervene in a given charge-transport pathway; and *N* + 1 is the electron-accepting purine nucleobase in the nucleic acid. *J* is the electron charge flux to the nucleic acid and/or other agent in the environment that sweeps away the electron once it arrives at site *N* + 1 (see main text). Thus, the occupation probability of this site is negligible at any time, and the backward rate $k_{N+1\to N}$ (in gray) does not appear in the corresponding master equation (Equation S25).

Procedures and Section S6 of Supplemental Information. The resulting rate constants are reported in Figure 3.

To demonstrate point (1), we built a kinetic model (see Figure 4 and Supplemental Information [Section S6]) to quantify the efficiency of the hole-transfer routes from the initially oxidized duplex to the $[4Fe4S]^{2+}$ cluster. The model is described more simply and equivalently in terms of electron transfer from $[4Fe4S]^{2+}$ to an oxidized duplex, which reduces the latter. Assuming the charge-hopping mechanism (which is a completely incoherent regime of charge conduction, with complete nuclear relaxation of the system between any CT process and the next one), the probabilities that the transferring electron charge is in the different redox sites shown in Figure 3 in any given CT route are given by the classical-type master equation

$$\begin{cases} \dfrac{dP_0}{dt} = -P_0 k_{0\to1} + P_1 k_{1\to0} \\ \dfrac{dP_n}{dt} = -P_n(k_{n\to n-1} + k_{n\to n+1}) + P_{n-1}k_{n-1\to n} + P_{n+1}k_{n+1\to n} \\ \dfrac{dP_{N+1}}{dt} = P_N k_{N\to N+1} - J. \end{cases} \qquad \text{(Equation 1)}$$

In the electron-hopping chain, $n = 0$ denotes the iron-sulfur cluster, $n = 1$ to N indicate the amino acid residues that can support the charge transport, and site $N + 1$ is the arrival nucleobase, which is in contact with the charge drain. $k_{n\to n'}$ is the rate constant for the electron-transfer step from site n to site n' (or, equivalently, for the converse hole-transfer step) and J is the charge flux out of site $N + 1$ (Figure 4). J and all occupation probabilities depend on t. We coupled Equation 1 with the time boundary conditions $P_0(0) = 1$, because the transferring electron is initially on the cluster (i.e., site 0 in Figure 4); $P_{N+1}(t) = 0$ for any t, because we describe the nucleic acid duplex together with nearby redox agents (e.g., oxidants) that may contribute to protein signaling as a charge drain that swipes away the transferred electron; and $\int_0^\infty J(t)dt = 1$, because the electron charge is finally delivered to the drain. This non-steady-state problem is further detailed and solved in Supplemental Information. The speed of charge flow through an electron-hopping route is measured by the mean residence time[37,38] of the transferring charge in the iron-sulfur cluster-protein complex, prior to its arrival at the nucleic acid. In Section S6 of Supplemental Information, we obtained the following expression for this time:

$$\tau = \sum_{n=0}^{N-1} \frac{1}{k_{n\to n+1}} \left(\sum_{j=0}^{N-n-1} \prod_{i=n+1}^{N-j} \frac{k_{i\to i-1}}{k_{i\to i+1}} + 1 \right) + \frac{1}{k_{N\to N+1}}. \qquad \text{(Equation 2)}$$

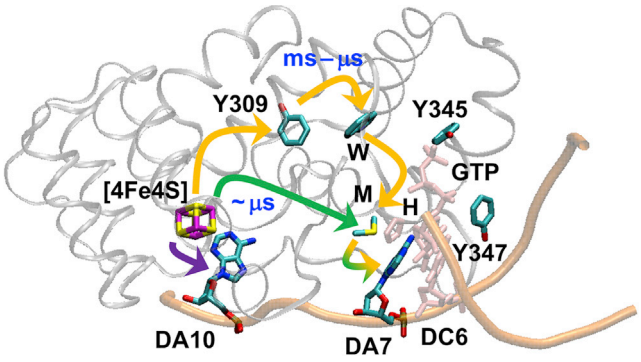

Figure 5. Electron-Transfer Routes from the p58c Protein to Nucleic Acid

The two most rapid electron-transfer paths from the p58c [4Fe4S] cluster to RNA/DNA (i.e., hole transfer in the opposite direction) are shown as green ([4Fe4S]-M307-DA7) and orange ([4Fe4S]-Y309-W327-M307-DA7) arrows. The timescale of the second route may range from ms to μs depending on the redox potentials of the Tyr and Trp residues. The purple arrow shows the fastest but unproductive electron transfer from [4Fe4S] to DA10 in the single-stranded DNA portion. H303 (denoted H), which is H-bonded to DA7, and DC6, which is paired to GTP, are in pink.

When all backward electron-transfer rates can be neglected, Equation 2 reduces to

$$\tau_{approx} \cong \sum_{n=0}^{N} \frac{1}{k_{n\to n+1}} \cdot (k_{n+1\to n} << k_{n\to n+1}, \quad 0 \le n < N), \qquad \text{(Equation 3)}$$

namely, the summation over the inverse rates for the individual CT steps in a given pathway. Inserting the rates of Figure 3 into Equation 2, we found that [4Fe4S]-M307-DA7 and [4Fe4S]-Y309-W327-M307-DA7 provide the fastest charge-hopping routes (see Figure 5 and Table 1).

For the CT route through M307, we obtained $\tau \cong$ 6 μs, while for the other CT route we found a τ value that ranges from milliseconds to microseconds depending on the characteristics of the CT through Tyr and Trp (see Figure 5 and Supplemental Information [Section S6]). These timescales (and especially the one for charge transport through M307 only) theoretically support the general validity of the experimental finding that the [4Fe4S] cluster can serve as an effective redox switch to modulate p58c-duplex interactions.[4,15] In fact, our result was obtained for a protein structure different from the mutated one used in O'Brien et al. [4] (therefore, a different specific CT pathway in the protein is at play) and is expected to be valid for any iron-sulfur protein with sufficient content of Tyr, Trp, and Met residues. Therefore, hole transfer from an oxidized RNA/DNA duplex to the $[4Fe4S]^{2+}$ cluster bound to p58c can occur on biologically relevant timescales, producing the $[4Fe4S]^{3+}$ cluster and strengthening the protein-duplex binding (thus preparing the initial state in signaling mechanism 1 of Figure 2A); and hole transfer can also occur from the duplex to p180c (allowed CT process in mechanism 1, which is denoted as step 3_h in Figure 1B).

The two different timescales for routes 2–4 in Table 1 depend on the way we treat the electron-transfer steps involving Tyr and Trp. For example, the oxidation potential for the Tyr residue is 0.93 V if the electron transfer is coupled to proton transfer to a residue nearby, Y-OH → Y-$O^{\cdot}$ + H^+ + e^- (here, differently from Table 1, Y denotes the Tyr without the hydroxyl group, and hence Y-OH denotes the full amino acid residue), while the oxidation potential is 1.38 V in the case of pure electron transfer,Y-OH → Y-$OH^{\cdot +}$ + e^-.[39,40] If the transferring proton has a tight H bond with a residue nearby, the short-range proton transfer is expected not to affect appreciably the electronic wave functions of Tyr. In this case, the CT process leading to the Tyr

Table 1. Mean Residence Time τ in the [4Fe4S]-Protein Complex, Its Approximate Value τ_{approx} and Lower Bound $\tau_>$ for the Mean Residence Time Corresponding to Electron Transfer to $[4Fe4S]^{3+}$ (Obtained as the Inverse of the Smallest Electron-Transfer Rate Constant Involved)

Electron-Transfer Route	τ_{approx} (s)[a]	τ (s)[b]	$\tau_>$ (s)
1: [4Fe4S]-M307-DA7	5.7×10^{-6}	5.7×10^{-6}	7.0×10^{20}
2: [4Fe4S]-Y309-W327-M307-DA7	8.6×10^{-6} 9.8×10^{-4}	8.6×10^{-6} 7.3×10^{-3}	6.7×10^{7} 8.8×10^{13}
3: [4Fe4S]-Y309-W327-Y345-GTP	3.0 4.2×10^{-2}	3.1 25	6.7×10^{7} 8.8×10^{13}
4: [4Fe4S]-Y309-W327-Y345-Y347-DG4	1.0×10^{2} 1.0×10^{2}	3.6×10^{6} 2.3×10^{2}	6.7×10^{7} 8.8×10^{13}

For each route in which Tyr and Trp are involved, the first (second) line corresponds to the first (second) value of oxidation potential in Table S1.

[a]From Equation 3.

[b]From Equation 2.

oxidation can be described approximately as pure electron transfer with an oxidation potential close to the value for proton-coupled electron transfer.[19] This is essentially the case in the crystal structure with PDB: 5F0Q (e.g., the N atom of His292 side chain is in H-bond configuration with the OH group of the Y309 side chain). Therefore, in our analysis, we described the electron-transfer steps through Tyr residues using the Marcus rate equation with 0.93 V and 1.38 V as limiting values for the oxidation potential, in order to show the robustness of our kinetic conclusions with respect to parameter choices. We similarly used two oxidation potential values for Trp, and these two values are much closer to each other than for the case of Tyr (see Table S1).

Note that the conclusions on the feasibility of the electron transfer from the initially reduced iron-sulfur cluster to the initially oxidized duplex and on the relative speed of the electron-transfer routes in Table 1 are both not changed using oxidation potential values that differ by almost 0.5 eV, which are reflected in accordingly large changes (compared to the thermal energy) in the activation free energy of Marcus' formula. Although the relative difference in τ for the electron-transfer routes to GTP and DG4 depends significantly on the oxidation potentials used for Tyr and Trp (and we cannot exclude the possibility that thermal fluctuations of the protein structure erase this difference), this difference is unessential to establish the feasibility of the electron-transfer mediation by the protein. In fact, using the structure with PDB: 5F0Q,[12] our kinetic model predicts that electron transfer to GTP (that is, hole transfer from the GTP to the iron-sulfur cluster) is slower by several orders of magnitude compared to the electron transfer to DA7, with τ in the range 3–25 s, and the electron transfer to DG4 through Y345 and Y347[4] is even slower, with τ in the range 10^2–10^6 s (Table 1).

The efficiencies of all charge-hopping routes depend on theoretical values of the reorganization energies for CT between protein residues (for which direct experimental information is currently unavailable), and could be influenced by fluctuations of the protein structure. However, these two factors cannot erase the large gap in speed between the CT paths to DA7 and to GTP or DG4 shown in Table 1 (while thermal fluctuations of the protein structure could produce appreciable relative changes in the rapidity of slow electron-transfer routes, such as routes 3 and 4). For example, although large thermal fluctuations could change the distances between redox partners for a time longer than the pertinent CT steps (thus causing appreciable changes in the effective CT distances and in the corresponding outer-sphere reorganization

energies), Marcus theory[36] implies a relatively weak dependence of the outer-sphere reorganization energy on the donor-acceptor distance, provided that this distance is much larger than the effective donor and acceptor radii. Thus, we expect that departures of the reorganization energies from the values estimated in the Supplemental Information by a significant fraction of eV are not likely. Furthermore, considering, for example, the CT steps that involve the frequently occurring Tyr and Trp residues (see Figure 3), the use of oxidation potentials that differ by a significant fraction of eV implies changes of similar magnitude in the reaction free energy for electron transfer to other residues, and these changes affect the electron-transfer rates more than similar changes in the reorganization energy would (because the reorganization energy, differently from the reaction free energy, is also contained in the denominator of Marcus' expression for the activation energy). Yet Table 1 shows the robustness of the conclusions with respect to the choice of Tyr and Trp oxidation potentials.

The above analysis does not rule out that, in a mutated protein, changes in p58 local folding[4,15] can significantly alter the Tyr positions and therefore the specific route that enables the fastest electron transfer from the iron-sulfur cluster to the nucleic acid.

CT Unidirectionality and [4Fe4S] Signaling Mechanisms

Importantly, while duplex-to-protein hole transfer is feasible irrespective of the system-dependent specific path, we find that the hole transfer in the opposite direction from $[4Fe4S]^{3+}$ to an initially neutral RNA/DNA duplex cannot occur on biologically relevant timescales (forbidden hole transfer from the p58c iron-sulfur cluster to the duplex in mechanism 1 of Figure 2A, which is denoted as step 1_h in Figure 1B). This conclusion is achieved without building a kinetic model for the protein-to-duplex hole transfer (which would require different boundary conditions), since at least one inverse electron-transfer rate in all routes of Figure 3 is much larger than any biologically relevant timescale (Table 1 and Supplemental Information [Section S6]) and makes the pertinent electron-transfer route much slower than the route in the opposite direction. Therefore, in Table 1 we only reported lower bounds for the mean residence times associated with the converse CT routes, obtained as the inverse rate constants for the most rate-limiting electron-transfer steps involved. The oxidation potentials of the redox-active species play an important role in preventing this hole transfer (which we assessed and quantified in terms of CT rates), and using the gamut of redox potential values in the literature cannot significantly affect the free energy scheme in Figure 2B and its implications for hole transfer (or excess electron transfer). While the currently available force fields for the [4Fe4S] cluster lead to significant distortions of the cluster (thus hindering accurate MD simulations of cluster-protein complexes) and the heterogeneous nature of the redox centers involved requires using different methods to compute electronic couplings, the $\tau_>$ values in Table 1 and their comparison with the corresponding "forward" τ values establish the unidirectional character of the hole transfer between the [4Fe4S] cluster and the duplex robustly with respect to any future computational refinements. An important implication of this unidirectionality is that, in mechanism 1 of Figure 2A, the p58c [4Fe4S] cluster cannot inject into the duplex the hole that must then traverse the nucleic acid and finally oxidize the [4Fe4S] cluster in p180c to accomplish signaling. However, if a hole is injected into the duplex by a nearby oxidant, this hole can then be transferred to the p180c cluster (allowed transition in mechanism 1). In fact, for hole transfer from the duplex to the $[4Fe4S]^{2+}$ cluster anchored to p180c, the redox-active moieties involved are the same as in the duplex-p58c complex: the [4Fe4S] cluster, nucleobases, and (depending on the relative orientation of p180c and p180core polymerase domains) the same types of amino acid residues. Thus, similar values of the free energy parameters are at play.

We now consider the possibility that the signaling between iron-sulfur proteins is mediated by transfer of an excess electron through the RNA/DNA duplex (signaling mechanism 2 of Figure 2A, which is represented by steps 1_e–3_e in Figure 1B): the initially reduced p180c iron-sulfur cluster donates an excess electron to an initially neutral duplex, which uses this electron to reduce the initially oxidized p58c iron-sulfur cluster.

Through-protein excess electron transfer from an anionic duplex to $[4Fe4S]^{3+}$ (step 3_e in Figure 1B) can occur on biologically relevant timescales on the basis of the redox potentials of the involved species (Tables S1 and S2; Figure 2B) and the localization properties of the diabatic electronic states in excess electron transfer. In fact, on average, the excess electron charge is expected to be more delocalized than the electron hole on a given redox-active moiety, and the reorganization energy value drops as the excess charge delocalizes.[41,42] Furthermore, the electronic coupling involved in an excess electron transfer step is expected to be larger, on average, than the electronic coupling for hole transfer between the same redox sites because of the greater delocalization of the diabatic electronic states. Given these considerations, we can assert the feasibility of excess electron transport from the anionic nucleic acid to the $[4Fe4S]^{3+}$ cluster in p58 (step 3_e in Figure 1B or process on the right in mechanism 2 of Figure 2) without repeating calculations analogous to those described above for the case of hole transfer.

Excess electron transfer from $[4Fe4S]^{2+}$ to the duplex (step 1_e in Figure 1B) is instead energetically unfavorable (forbidden CT step in mechanism 2 of Figure 2A, and transition d in Figure 2B). The redox-active Tyr, Trp, and Met residues (note that methionine sulfoxide is usually the starting compound in Met reduction[43]) cannot support excess electron transfer from the iron-sulfur cluster to the nucleic acid. This process is kinetically unfeasible even if the $[4Fe4S]^{2+}$ cluster in p180c comes into direct contact with the duplex attached to p180c. By combining crystallographic information with density functional theory (DFT) electronic structure analysis of the excess electron distribution on the guanine near the p180c iron-sulfur cluster, we estimated a minimum center-to-center distance of about 8 Å between the guanine and the cluster, and a maximum electron-transfer rate on the order of 10^{-7} s^{-1} (see lower panel in Table S7). Accordingly, redox signaling cannot be mediated exclusively by excess electron transfer through the duplex. We can state this result because of the kinetic impossibility of step 1_e shown in Figure 1B, irrespective of the computational validation (not provided in this study) of our arguments in support of the kinetic feasibility of step 3_e. However, our results do not exclude that a reducing agent (such as, e.g., glutathione) in the surrounding environment can donate the electron to the duplex and thus enable mechanism 2.

Mechanism 3 in Figure 2A envisages signaling by direct CT (either hole transfer or excess electron transfer) between the two [4Fe4S] clusters, while p58c holds the template/primer during its handoff to Polα.[12] In this scenario, the hole transfer should occur by superexchange, since the cluster-to-protein hole hopping is energetically unfavorable (Figure 2B). Excess electron transfer should also occur by superexchange, since the CT step from the cluster to any of the redox-active amino acids is energetically unfeasible. Direct CT between the two [4Fe4S] clusters is expected to change the relative strengths of p58c and p180c binding to the duplex,[4] promoting primer transition. Charge self-exchange between the [4Fe4S] clusters at the distance shown in Figure 1 cannot occur on a biologically relevant timescale. However, the flexibility of the p58c-$p58_N$ linker,[12,44] and substantial conformational

changes during primer synthesis,[12] might bring the [4Fe4S] clusters sufficiently close to each other to enable direct CT. Our analysis (top panel in Table S7) establishes a maximum inter-cluster distance of ~12.5 Å for the occurrence of direct hole transfer. Testing the feasibility of this signaling mechanism requires additional structural data and, from a theoretical perspective, the development of accurate methods to calculate free energy and coupling parameters for CT between [4Fe4S] clusters. We computed the electronic couplings between [4Fe4S] clusters (Tables S4 and S7) with a method that only includes a few low-energy electronic states of the iron-sulfur clusters.[45] However, a recent theoretical study accurately describes a large density of [4Fe4S] electronic states that can contribute to the electronic coupling between the clusters,[46] thus increasing the electronic transmission coefficient in the electron-transfer rate and correspondingly growing the range of inter-cluster distances that would enable direct CT.

Mechanism 4 in Figure 2A does not require CT between [4Fe4S] clusters, but it again relies on the connection between [4Fe4S] cluster oxidation and DNA binding. After p58c binding to the duplex, the latter donates an electron to an oxidant nearby (Figure 2A, mechanism 4, middle panel). The Polα [4Fe4S] cluster then reduces and binds the duplex, displacing the primase by steric or other structural interactions (Figure 2A, mechanism 4, bottom panel). The necessary presence of an oxidant species makes signaling mechanism 4 more sensitive to oxidant concentration than mechanism 3, thus offering a means to distinguish, experimentally, between the two mechanisms, if they are viable.

In conclusion, we demonstrate that protein-mediated hole transfer or excess electron transfer between an iron-sulfur cluster and a nucleic acid duplex is always possible in one direction, on a microsecond timescale, irrespective of the specific charge-hopping pathway used to accomplish the CT. This finding solves a main point of debate in the recent literature,[4,13–15] showing that the redox "communication" between the [4Fe4S] cluster and nucleic acid is, indeed, possible[15] irrespective of the specific protein pathway involved.

However, the demonstrated one-directionality in CT between protein iron-sulfur cluster and nucleic acid duplex sets clear conditions on the possible mechanisms of redox signaling between [4Fe4S] proteins, ruling out any mechanism in which the signaling is exclusively mediated by DNA charge transport, thus requiring CT in both [4Fe4S]-to-DNA and DNA-to-[4Fe4S] directions. The free energy landscape in Figure 2B was clearly not sufficient to establish the CT one-directionality, which depends on the actual participation of the high-potential amino acid residues in the most rapid charge-transport paths and on the resulting effective CT rates, as compared with a reasonable lower bound of a millisecond timescale for the occurrence of biological processes. Our structural analysis (with the identification of the redox-active amino acids in "strategic" positions), kinetic study of the different charge-transport routes (with the identification of the most rapid routes), and quantification of the rapidity of such CT pathways allowed us to establish in an unquestionable way the one-directional character of the CT between [4Fe4S] cluster and nucleic acid. Future theoretical-computational refinements cannot affect this major conclusion, although they would improve our quantitative knowledge of the protein-mediated CT in the allowed direction. For example, while route 2 (Table 1 and Figure 5) is kinetically feasible within a biologically relevant timescale irrespective of the set of oxidation potential values used, the difference in rapidity between routes 1 and 2 can be significantly influenced by the CT parameters. In particular, future studies of hole transfer through Tyr and Trp residues could

help us to narrow the range of timescales for CT route 2 provided in this study. Therefore, future computational refinements would enable a more accurate comparison between the efficiencies of routes 1 and 2, which, in turn, would enable theoretical predictions on the possible effects of mutations on the relative rapidity of such CT paths.

We identified the only feasible classes of mechanisms for redox signaling between [4Fe4S] proteins (mechanisms 1–4 in Figure 2A) as those compatible with the above finding and with the dependence of the protein-DNA binding affinity on the oxidation state of the [4Fe4S] cluster.[4,9] The proposed signaling mechanisms frame future studies on primer synthesis and, more generally, on protein communication via redox signaling between [4Fe4S] clusters. All mechanisms are compatible with the current knowledge of human primosome structure and dynamics,[12] and also support the potential for [4Fe4S] cluster redox signaling in biology.[4]

More generally, our findings help to narrow the search for functional CT processes in DNA replication and lesion detection/repair and can assist in the design of primosome inhibitors that may be of use for arresting DNA replication in cancer cells.[3] Discrimination among the mechanisms described in Figure 2A demands future experimental investigations that provide the missing structural information and study the protein-nucleic acid complex under different oxidation/reduction environmental conditions (for example, the two protein-DNA CT steps in mechanisms 1 and 2 could be studied separately, using DNA-mediated electrochemistry as in O'Brien et al., [4] with different concentrations of oxidants or reductants), thus producing new fundamental understanding of redox signaling processes between iron-sulfur proteins relevant to biomedicine.

Theoretical and Computational Procedures

We docked a [4Fe4S] cluster to ZBS1 of p180c using the AutoDock Vina program,[47] the protein crystal structure with PDB: 5EXR,[12] and cluster internal coordinates from the crystal structure with PDB: 5F0Q.[12] The docking provided the missing structural information for the system in Figure 1A. Tunneling pathways analysis[48,49] using the Pathways 1.2 plugin[50] for VMD[51] followed by inspection of the redox-active protein residues aided the identification of the potentially fast electron-hopping routes between the p58c [4Fe4S] cluster and nucleobases in the complexed RNA/DNA (Figure 3). The calculation of Marcus rate constant (Equation S20) for each CT step in Figure 3 required knowledge of the pertinent reaction free energy, reorganization (free) energy, and donor-acceptor electronic coupling.[36] The reaction free energy was derived from the redox potentials of donor and acceptor, which were obtained from the literature and also derived using Equation S7.[28] The missing reduction potentials were obtained from Equation S8,[28] after DFT calculation of the needed vertical electron affinities using the M06-HF,[52,53] M06-2X,[52,54] and PBE0[55] hybrid meta density functionals and the cc-pVTZ basis set. The reorganization energies were obtained from Equations S3, S5,[36] S6, and S22. When needed, the effective radius of the charge donor/acceptor was obtained from Equation S21, after DFT calculation of the atomic charges. The electronic couplings were evaluated using semiempirical methods (Equations S9[56] and S10[45]) and gas-phase DFT implementations of Equation S11[30,57] with the M11 density functional[58] and the 6-311g** basis set. The effect of the protein medium on the gas-phase electronic couplings was introduced through Equation S16, which was developed exploiting the average packing density model.[59,60] This is to be considered as a zero-order correction for the effect of the protein on the tunneling barriers and therefore on the electronic couplings calculated for the gas-phase models. This approach is amenable to future improvements,

beginning with specific evaluations of the protein average packing densities. However, refinements of the method are expected to produce variations of the couplings within the range set, for example, by the comparison of the results from Equation S9 and DFT, and clearly cannot affect any of the conclusions based on the huge differences between the forward and backward residence times presented in Table 1. The electronic couplings between the iron-sulfur cluster and redox partners were computed using Equation S18. The resulting CT rate constants were inserted into Equation 2 (which is the solution of the kinetic model shown in Figure 4; see the derivation of this equation in Section S6 of Supplemental Information) to obtain the mean residence times of the charge in the [4Fe4S]-protein system, along the different CT routes identified in Figure 3. For the case of excess electron transfer, the maximum rate constant for direct CT from the $[4Fe4S]^{2+}$ cluster to a guanine was evaluated as detailed in Supplemental Information Section S6, after DFT calculation of the guanine effective radius and inner-sphere reorganization energy (see lower panels of Tables S7 and S8).

EXPERIMENTAL PROCEDURES

Full experimental procedures are provided in the Supplemental Information, including details of the docking of the [4Fe4S] cluster to the p180c protein and on the protein-nucleic acid complex structure (including a map of the redox-active amino acid residues); calculation of the CT parameters (free energies and electronic couplings) and the CT rates for all redox couples involved in the charge transfer between p58c and the RNA/DNA duplex; an electron tunneling pathway analysis; and the development of a kinetic model that quantifies the rapidity of the different CT routes.

SUPPLEMENTAL INFORMATION

Supplemental Information includes Supplemental Experimental Procedures, six figures, and eight tables and can be found with this article online at https://doi.org/10.1016/j.chempr.2018.09.026.

ACKNOWLEDGMENTS

We thank Profs. Harry B. Gray and Carlos E. Crespo-Hernández for helpful discussions and Dr. Tomasz Janowski and the Duke Compute Cluster (DCC) Team for technical support. Computations were performed using the DCC and ET clusters at Duke University. We acknowledge the National Institutes of Health (grant GM-48043) for support of this research.

AUTHOR CONTRIBUTIONS

All authors discussed the results, commented on the manuscript, and contributed to its writing. In addition: R.D.T. carried out computations and analysis of results; B.J.G.R. contributed to computations; R.D.F. contributed to the pathway product analysis; A.M. conceived and designed the research, developed the kinetic model, contributed to computations, and headed the analysis of results and the manuscript writing.

DECLARATION OF INTERESTS

The authors declare no competing interests.

Received: July 31, 2018
Revised: September 24, 2018
Accepted: September 27, 2018
Published: October 25, 2018; corrected online: May 29, 2019

REFERENCES AND NOTES

1. Roche, B., Aussel, L., Ezraty, B., Mandin, P., Py, B., and Barras, F. (2013). Iron/sulfur proteins biogenesis in prokaryotes: formation, regulation and diversity. Biochim. Biophys. Acta *1827*, 455–469.
2. Rouault, T.A. (2015). Mammalian iron-sulphur proteins: novel insights into biogenesis and function. Nat. Rev. Mol. Cell Biol. *16*, 45–55.
3. Fuss, J.O., Tsai, C.-L., Ishida, J.P., and Tainer, J.A. (2015). Emerging critical roles of Fe-S clusters in DNA replication and repair. Biochim. Biophys. Acta *1853*, 1253–1271.
4. O'Brien, E., Holt, M.E., Thompson, M.K., Salay, L.E., Ehlinger, A.C., Chazin, W.J., and Barton, J.K. (2017). The [4Fe4S] cluster of human DNA primase functions as a redox switch using DNA charge transport. Science *355*, eaag1789.
5. Boon, E.M., Livingston, A.L., Chmiel, N.H., David, S.S., and Barton, J.K. (2003). DNA-mediated charge transport for DNA repair. Proc. Natl. Acad. Sci. U S A *100*, 12543–12547.
6. Boal, A.K., Genereux, J.C., Sontz, P.A., Gralnick, J.A., Newman, D.K., and Barton, J.K. (2009). Redox signaling between DNA repair proteins for efficient lesion detection. Proc. Natl. Acad. Sci. U S A *106*, 15237–15242.
7. Bartels, P.L., Zhou, A., Arnold, A.R., Nuñez, N.N., Crespilho, F.N., David, S.S., and Barton, J.K. (2017). Electrochemistry of the [4Fe4S] cluster in base excision repair proteins: tuning the redox potential with DNA. Langmuir *33*, 2523–2530.
8. Grodick, M.A., Segal, H.M., Zwang, T.J., and Barton, J.K. (2014). DNA-mediated signaling by proteins with 4Fe-4S clusters is necessary for genomic integrity. J. Am. Chem. Soc. *136*, 6470–6478.
9. Tse, E.C.M., Zwang, T.J., and Barton, J.K. (2017). The oxidation state of [4Fe4S] clusters modulates the DNA-binding affinity of DNA repair proteins. J. Am. Chem. Soc. *139*, 12784–12792.
10. Netz, D.J.A., Stith, C.M., Stümpfig, M., Köpf, G., Vogel, D., Genau, H.M., Stodola, J.L., Lill, R., Burgers, P.M.J., and Pierik, A.J. (2012). Eukaryotic DNA polymerases require an iron-sulfur cluster for the formation of active complexes. Nat. Chem. Biol. *8*, 125–132.
11. Arnold, A.R., Grodick, M.A., and Barton, J.K. (2016). DNA charge transport: from chemical principles to the cell. Cell. Chem. Biol. *23*, 183–197.
12. Baranovskiy, A.G., Babayeva, N.D., Zhang, Y., Gu, J., Suwa, Y., Pavlov, Y.I., and Tahirov, T.H. (2016). Mechanism of concerted RNA-DNA primer synthesis by the human primosome. J. Biol. Chem. *291*, 10006–10020.
13. Baranovskiy, A.G., Babayeva, N.D., Zhang, Y., Blanco, L., Pavlov, Y.I., and Tahirov, T.H. (2017). Comment on "The [4Fe4S] cluster of human DNA primase functions as a redox switch using DNA charge transport". Science *357*, eaan2396.
14. Pellegrini, L. (2017). Comment on "The [4Fe4S] cluster of human DNA primase functions as a redox switch using DNA charge transport". Science *357*, eaan2954.
15. O'Brien, E., Holt, M.E., Thompson, M.K., Salay, L.E., Ehlinger, A.C., Chazin, W.J., and Barton, J.K. (2017). Response to comments on "The [4Fe4S] cluster of human DNA primase functions as a redox switch using DNA charge transport". Science *357*, eaan2762.
16. Vaithiyalingam, S., Warren, E.M., Eichman, B.F., and Chazin, W.J. (2010). Insights into eukaryotic DNA priming from the structure and functional interactions of the 4Fe-4S cluster domain of human DNA primase. Proc. Natl. Acad. Sci. U S A *107*, 13684–13689.
17. Baranovskiy, A.G., Zhang, Y.B., Suwa, Y., Gu, J.Y., Babayeva, N.D., Pavlov, Y.I., and Tahirov, T.H. (2016). Insight into the human DNA primase interaction with template-primer. J. Biol. Chem. *291*, 4793–4802.
18. Baranovskiy, A.G., Babayeva, N.D., Suwa, Y., Gu, J., Pavlov, Y.I., and Tahirov, T.H. (2014). Structural basis for inhibition of DNA replication by aphidicolin. Nucleic Acids Res. *42*, 14013–14021.
19. Gray, H.B., and Winkler, J.R. (2015). Hole hopping through tyrosine/tryptophan chains protects proteins from oxidative damage. Proc. Natl. Acad. Sci. U S A *112*, 10920–10925.
20. Winkler, J.R., and Gray, H.B. (2015). Electron flow through biological molecules: does hole hopping protect proteins from oxidative damage? Q. Rev. Biophys. *48*, 411–420.
21. Khan, A. (2013). Reorganization, activation and ionization energies for hole transfer reactions through inosine-cytosine, 2-aminopurine-thymine, adenine-thymine, and guanine-cytosine base pairs: a computational study. Comput. Theor. Chem. *1013*, 136–139.
22. Kubař, T., and Elstner, M. (2009). Solvent reorganization energy of hole transfer in DNA. J. Phys. Chem. B *113*, 5653–5656.
23. Siriwong, K., and Voityuk, A.A. (2012). Electron transfer in DNA. WIREs Comput. Mol. Sci. *2*, 780–794.
24. Renaud, N., Berlin, Y.A., Lewis, F.D., and Ratner, M.A. (2013). Between superexchange and hopping: an intermediate charge-transfer mechanism in Poly(A)-Poly(T) DNA hairpins. J. Am. Chem. Soc. *135*, 3953–3963.
25. Zhang, Y., Liu, C., Balaeff, A., Skourtis, S.S., and Beratan, D.N. (2014). Biological charge transfer via flickering resonance. Proc. Natl. Acad. Sci. U S A *111*, 10049–10054.
26. Steenken, S., and Jovanovic, S.V. (1997). How easily oxidizable is DNA? One-electron reduction potentials of adenosine and guanosine radicals in aqueous solution. J. Am. Chem. Soc. *119*, 617–618.
27. Steenken, S., Jovanovic, S.V., Bietti, M., and Bernhard, K. (2000). The trap depth (in DNA) of 8-oxo-7,8-dihydro-2′deoxyguanosine as derived from electron-transfer equilibria in aqueous solution. J. Am. Chem. Soc. *122*, 2373–2374.
28. Crespo-Hernández, C.E., Close, D.M., Gorb, L., and Leszczynski, J. (2007). Determination of redox potentials for the Watson-Crick base pairs, DNA nucleosides, and relevant nucleoside analogues. J. Phys. Chem. B *111*, 5386–5395.
29. Rosch, N., and Voityuk, A.A. (2004). Quantum chemical calculation of donor-acceptor coupling for charge transfer in DNA. Top. Curr. Chem. *237*, 37–72.
30. Migliore, A. (2009). Full-electron calculation of effective electronic couplings and excitation energies of charge transfer states: application to hole transfer in DNA π-stacks. J. Chem. Phys. *131*, 114113.
31. Migliore, A., Corni, S., Varsano, D., Klein, M.L., and Di Felice, R. (2009). First principles effective electronic couplings for hole transfer in natural and size-expanded DNA. J. Phys. Chem. B *113*, 9402–9415.
32. Blancafort, L., and Voityuk, A.A. (2006). CASSCF/CAS-PT2 study of hole transfer in stacked DNA nucleobases. J. Phys. Chem. A *110*, 6426–6432.
33. Blancafort, L., and Voityuk, A.A. (2007). MS-CASPT2 calculation of excess electron transfer in stacked DNA nucleobases. J. Phys. Chem. A *111*, 4714–4719.
34. Kelley, S.O., and Barton, J.K. (1999). Electron transfer between bases in double helical DNA. Science *283*, 375–381.
35. Guo, X., Gorodetsky, A.A., Hone, J., Barton, J.K., and Nuckolls, C. (2008). Conductivity of a single DNA duplex bridging a carbon nanotube gap. Nat. Nanotechnol. *3*, 163–167.
36. Marcus, R.A., and Sutin, N. (1985). Electron transfers in chemistry and biology. Biochim. Biophys. Acta *811*, 265–322.
37. Bar-Haim, A., and Klafter, J. (1998). On mean residence and first passage times in finite one-dimensional systems. J. Chem. Phys. *109*, 5187–5193.
38. Cao, J. (2011). Michaelis-Menten equation and detailed balance in enzymatic networks. J. Phys. Chem. B *115*, 5493–5498.
39. Tommos, C., and Babcock, G.T. (2000). Proton and hydrogen currents in photosynthetic water oxidation. Biochim. Biophys. Acta *1458*, 199–219.
40. Schlodder, E., Cetin, M., and Lendzian, F. (2015). Temperature dependence of the oxidation kinetics of Tyr(Z) and Tyr(D) in oxygen-evolving photosystem II complexes throughout the range from 320 K to 5 K. Biochim. Biophys. Acta *1847*, 1283–1296.
41. Petersen, R.A., and Evans, D.H. (1987). Heterogeneous electron transfer kinetics for a variety of organic electrode reactions at the mercury-acetonitrile interface using either tetraethylammonium perchlorate or tetraheptylammonium perchlorate electrolyte. J. Electroanal. Chem. *222*, 129–150.
42. Migliore, A., and Nitzan, A. (2011). Nonlinear charge transport in redox molecular junctions: a Marcus perspective. ACS Nano *5*, 6669–6685.
43. Kim, G., Weiss, S.J., and Levine, R.L. (2014). Methionine oxidation and reduction in proteins. Biochim. Biophys. Acta *1840*, 901–905.

44. Baranovskiy, A.G., Zhang, Y., Suwa, Y., Babayeva, N.D., Gu, J., Pavlov, Y.I., and Tahirov, T.H. (2015). Crystal structure of the human primase. J. Biol. Chem. *290*, 5635–5646.

45. Voityuk, A.A. (2010). Electron transfer between [4Fe-4S] clusters. Chem. Phys. Lett. *495*, 131–134.

46. Sharma, S., Sivalingam, K., Neese, F., and Chan, G.K. (2014). Low-energy spectrum of iron-sulfur clusters directly from many-particle quantum mechanics. Nat. Chem. *6*, 927–933.

47. Trott, O., and Olson, A.J. (2010). AutoDock Vina: improving the speed and accuracy of docking with a new scoring function, efficient optimization and multithreading. J. Comput. Chem. *31*, 455–461.

48. Beratan, D.N., Betts, J.N., and Onuchic, J.N. (1992). Tunneling pathway and redox-state-dependent electronic couplings at nearly fixed distance in electron-transfer proteins. J. Phys. Chem. *96*, 2852–2855.

49. Jones, M.L., Kurnikov, I.V., and Beratan, D.N. (2002). The nature of tunneling pathway and average packing density models for protein-mediated electron transfer. J. Phys. Chem. A *106*, 2002–2006.

50. Balabin, I.A., Hu, X.Q., and Beratan, D.N. (2012). Exploring biological electron transfer pathway dynamics with the pathways Plugin for VMD. J. Comput. Chem. *33*, 906–910.

51. Humphrey, W., Dalke, A., and Schulten, K. (1996). VMD: visual molecular dynamics. J. Mol. Graph. *14*, 33–38.

52. Zhao, Y., and Truhlar, D.G. (2008). The M06 suite of density functionals for main group thermochemistry, thermochemical kinetics, noncovalent interactions, excited states, and transition elements: two new functionals and systematic testing of four M06-class functionals and 12 other functionals. Theor. Chem. Acc. *120*, 215–241.

53. Zhao, Y., and Truhlar, D.G. (2006). Density functional for spectroscopy: no long-range self-interaction error, good performance for Rydberg and charge-transfer states, and better performance on average than B3LYP for ground states. J. Phys. Chem. A *110*, 13126–13130.

54. Zhao, Y., and Truhlar, D.G. (2008). Density functionals with broad applicability in chemistry. Acc. Chem. Res. *41*, 157–167.

55. Adamo, C., and Barone, V. (1999). Toward reliable density functional methods without adjustable parameters: the PBE0 model. J. Chem. Phys. *110*, 6158–6170.

56. Hopfield, J.J. (1974). Electron transfer between biological molecules by thermally activated tunneling. Proc. Natl. Acad. Sci. U S A *71*, 3640–3644.

57. Migliore, A. (2011). Nonorthogonality problem and effective electronic coupling calculation: application to charge transfer in π-stacks relevant to biochemistry and molecular electronics. J. Chem. Theor. Comput. *7*, 1712–1725.

58. Peverati, R., and Truhlar, D.G. (2011). Improving the accuracy of hybrid meta-GGA density functionals by range separation. J. Phys. Chem. Lett. *2*, 2810–2817.

59. Moser, C.C., Keske, J.M., Warncke, K., Farid, R.S., and Dutton, P.L. (1992). Nature of biological electron transfer. Nature *355*, 796–802.

60. Page, C.C., Moser, C.C., Chen, X.X., and Dutton, P.L. (1999). Natural engineering principles of electron tunnelling in biological oxidation-reduction. Nature *402*, 47–52.